



HAL
open science

Influence of the chain extender of a segmented polyurethane on the properties of polyurethane-modified asphalt blends

Raïssa Gallu, Françoise Méchin, Jean-François Gérard, Florent Dalmas

► To cite this version:

Raïssa Gallu, Françoise Méchin, Jean-François Gérard, Florent Dalmas. Influence of the chain extender of a segmented polyurethane on the properties of polyurethane-modified asphalt blends. *Construction and Building Materials*, 2022, 328, pp.127061. 10.1016/j.conbuildmat.2022.127061 . hal-03604474

HAL Id: hal-03604474

<https://hal.science/hal-03604474>

Submitted on 10 Mar 2022

HAL is a multi-disciplinary open access archive for the deposit and dissemination of scientific research documents, whether they are published or not. The documents may come from teaching and research institutions in France or abroad, or from public or private research centers.

L'archive ouverte pluridisciplinaire **HAL**, est destinée au dépôt et à la diffusion de documents scientifiques de niveau recherche, publiés ou non, émanant des établissements d'enseignement et de recherche français ou étrangers, des laboratoires publics ou privés.

Influence of the chain extender of a segmented polyurethane on the properties of polyurethane-modified asphalt blends

Raïssa Gallu^{1,2*}, Françoise Méchin¹, Jean-François Gérard¹, Florent Dalmas^{2*}

¹ Univ Lyon, CNRS, UMR 5223, Ingénierie des Matériaux Polymères, Université Claude Bernard Lyon 1, INSA Lyon, Université Jean Monnet, F-69621 Villeurbanne Cedex, France

² Univ Lyon, INSA Lyon, CNRS, MATEIS, UMR5510, F-69621, Villeurbanne, France.

ABSTRACT

This paper reviews the influence of the hard segment (HS) chemical structure on the properties of thermoplastic polyurethanes based on dimer fatty acid soft segments, and on their resulting blends with bitumen. Three types of hard segments were used which consist in 4,4'-methylene bis(phenyl isocyanate) (MDI) reacted either with 1,4-butanediol (BDO), 1,4:3,6-dianhydro D-sorbitol (isosorbide) or 2-ethyl-1,3-hexanediol (EHDO). The characterization of thermoplastic polyurethanes (TPUs) containing 13 wt% HS was conducted by differential scanning calorimetry, dynamic mechanical analysis, Hansen solubility parameters measurements and morphology analysis. The use of Hansen solubility parameters combined with thermal and swelling analyses provides information about the quality of phase separation occurring in the neat TPUs. Phase separation depends on the hard segments used and on their ability to self-organize within crystalline structures. Morphology analysis and swelling measurements of the TPU blended with bitumen by fluorescence microscopy show that the swelling of the polymer is highly dependent on the quality of phase separation between soft and hard segments in the pure polymer as well as on the compatibility of these segments with bitumen. Highly phase separated TPUs offer elasticity improvement to the bituminous blend.

Keywords. polymer-modified bitumen; thermoplastic polyurethane, Hansen solubility parameters, morphology, mechanical properties.

1. INTRODUCTION

The properties of a polymer-modified bitumen are highly dependent on the polymer used to manufacture the blend, due to a variation of affinity of bitumen with the polymer. As a result, morphology differences can come up whether e.g. the standard copolymer modifier poly(styrene-*b*-butadiene-*b*-styrene) (SBS), poly(ethylene-co-vinyl acetate) (EVA) or poly(ethylene-co-butyl acrylate) (EBA) are used¹. The nature of the polymer is assumed to be a key factor in the modification of bitumen. Indeed, bitumen can either present good compatibility with the polymer, as an example with polyethylene sulfide, only partial compatibility such as with SBS copolymer, or bad compatibility like with polyether sulfone².

Furthermore, literature has revealed that for a same (co)polymer nature, the difference of either composition, (i.e. for block copolymers the ratio of soft:hard blocks) or macromolecular architecture affects the viscoelastic properties of the polymer-modified bitumen blend. Indeed, for linear SBS copolymers, the optimum polymer composition for bitumen modification typically is a styrene:butadiene ratio of 30:70³, and for EVA copolymers a content of 18% of vinyl acetate⁴. Similarly, for a SBS copolymer, the architecture of the polymer, either radial or linear, leads to compatibility differences with the bitumen⁵. Indeed, during the manufacturing of a SBS-modified bitumen, the polybutadiene blocks are preferentially swollen by the light fractions of bitumen while the polystyrene blocks remain poorly swollen. This leads to a globally discrete swelling of the polymer. This swelling governs the morphology of the blend: for a given amount of SBS copolymer, low styrene to butadiene ratios induce highly swollen, bigger and more polydisperse polymer domains. At the same time, increasing the global amount of SBS copolymer in the blend turns the dispersed SBS-rich phase into a co-continuous SBS-rich phase after phase inversion that usually occurs close to 6 wt% SBS for linear SBS^{1,6}; therefore, swelling is directly responsible for this crucial feature that is phase inversion. It results in a change in viscoelastic properties of the SBS-modified bitumen, where the viscous behavior observed before phase inversion changes to an elastomeric mechanical behavior beyond phase inversion⁷.

Radial SBS is more favorable than linear SBS as it allows the formation of a continuous network in bitumen due to higher swelling, and leads to a blend with pronounced elastic response. Others reported on polyethylene-based polymers the importance of the polymer crystallinity as well as polarity, which informs on the bitumen-polymer interactions⁸. They showed that polymers having crystalline particles in their structure lead to blends with higher elastic response⁸.

In recent years, polyurethane polymers have gained importance in bitumen modification, and have become a competitive polymer to the usual polymers used for bitumen modification in roofing applications or road pavements. The interest in polyurethanes or more specifically in thermoplastic polyurethanes (TPU) comes from the versatility of those polymers, constituted with a polyol, a diisocyanate and a chain extender. This particular formulation results in more or less alternating soft (polyol) and hard (diisocyanate/chain extender) blocks. The variation of the soft and hard block architecture leads to change the thermodynamics within the two blocks of the polyurethane, as simply illustrated with the variation of the polyol nature (e.g. polybutadiene, polypropylene, or poly(tetramethylene oxide) [PTMO] exhibit different solubility parameters^{9,10}). The degree of phase segregation in the polyurethane as described by Camberlin and Pascault¹⁰ based on thermal analysis and discussed in a previous work¹¹ depends on the interactions between soft and hard blocks. They have shown a variation in the Flory-Huggins interaction parameter χ in the polyurethane when changing the soft segment¹⁰. Similarly, weaker interactions between soft and hard blocks provide a better phase segregation as shown with polyurethanes made from MDI and polyester vs polyether polyols^{12,13} where the polyether polyol contributes to decrease the interactions.

However, all three building blocks can impart the properties of the polymer. Indeed, the properties of the hard segments, as well as those of the segmented polymers clearly vary when changing the chain extender^{14,15}. The occurrence of strong H bond-type interactions within the hard segment is particularly related to the resulting thermal properties. For example, literature reported differences in morphology and thermal properties (such as glass transition temperature, crystallization ability and potential melting temperature) for hard segments made from 4,4'-diphenylmethane diisocyanate (MDI) with chain extenders of different chemical and/or spatial structures such as 1,4-butanediol (BDO), hydroquinone bis(2-hydroxyethyl) ether (HQEE)¹⁶, isosorbide and others¹⁴, also when varying their chain length e.g. with ethylene glycol, BDO, or 1,6-hexanediol^{17,18}, or even when comparing diols with odd and even numbers of methylene groups^{19,20}. Table 1 shows the thermal properties of some hard segments reported in the literature for various TPUs as a function of the chain extender used.

Table 1. Observed thermal properties of some hard segments used in thermoplastic polyurethanes (T_g = glass transition temperature; T_m = melting temperatures associated with high temperature endotherms)

	T_g (°C)	T_m (°C)
MDI-BDO ^{14,16}	107	198-225-240
MDI-HQEE ^{14,16}	98	215-245
MDI-CHDM ^{14,16}	134	190-210
MDI-NPG ^{14,16}	94	-
MDI-isosorbide ^{14,16}	187	235
MDI-HDO ²⁰	-	180-190
MDI-PDO ²⁰	-	210-225
MDI-EDO ²⁰	-	245-260

BDO : 1,4-butanediol ; HQEE : bis(β -hydroxyethyl) hydroquinone ; CHDM : 1,4-bis(hydroxymethyl) cyclohexane ; NPG : neopentyl glycol ; HDO : 1,6-hexanediol ; PDO : 1,3-propanediol ; EDO : ethylene glycol

Briefly, changing the architecture of the building blocks used to prepare the TPU leads to varying compatibility between the soft and the hard blocks, and consequently to polymers with different properties^{9,15}. However apart from the chemical composition, several other parameters impart the properties of the TPU, such as the block molar mass and the soft:hard block ratio.

Finally, the soft and hard block respective contents, as well as the compatibility between the blocks, or in other words the degree of phase separation, impact the mechanical properties of the TPU. The hard segment content plays a key role in the resulting mechanical properties of the polyurethane^{21,22}. A number of studies reported that increasing the hard segment content leads to an increase in the modulus of the polymer^{11,16,23}.

In our earlier work, we have shown that the behavior of TPUs in bitumen was quite similar to that of block copolymers such as SBS²⁴. Indeed, at low polymer content, a viscous blend presenting a morphology with dispersed TPU-rich phases was replaced beyond phase inversion by the appearance of a continuous TPU-rich phase governing the mechanical properties and conferring elasticity to the blend as long as the hard segment content was high enough to maintain an elastic behavior in the swollen TPU phase²⁴. As for SBS block copolymers with polystyrene domains, the hard nanodomains in TPU composed of MDI/BDO hard segments have revealed reduced compatibility with bitumen^{11,24}, characterized by a decrease in the whole

polymer swelling. However, literature shows that at high polymer content, the mechanical properties of the bitumen-polymer blends are governed by the polymer rich-phase, and in the case of TPU, the versatility of the polymer architecture can give rise to various mechanical properties for the blend, as anticipated from the various properties of the polymers themselves. The present study aims to understand the influence of the hard segment chemical composition and more specifically of the chain extender nature on the morphology and rheological properties of TPU-modified bitumen blends. Three chain extenders were used to synthesize TPUs and the properties of the polymers are discussed before blending with bitumen. Phase separation in the polymer is discussed regarding the chain extender used by means of Hansen solubility parameters tool, differential scanning calorimetry and microscopy analyses. Fluorescence microscopy observations of the blend are then conducted to analyze morphology and swelling of the polymer in bitumen. Finally, relationships are established between the polymer properties, swelling in bitumen based on its compatibility and the blend rheological properties.

2. EXPERIMENTAL SECTION

2.1. Materials

A 160/220 grade bitumen (sourced from the Mineraloel Raffinerie Oberrhein GmbH & Co in Karlsruhe, Germany) was used to make the blend with the TPU. The composition of this bitumen in SARA fractions consists in 10% saturates, 62% aromatics, 15.5% resins and 12.5% asphaltenes. This bitumen is characterized by a ring and ball softening temperature between 35°C and 43°C and a needle penetration of 176 1/10 mm at 25°C.

The TPUs are synthesized using a fatty acid derived polyester polyol, Radia 7285 (P3000) having a molar mass of 3200 g.mol⁻¹ supplied by Oleon Co. The chain extenders, 1,4-butanediol (BDO), 1,4:3,6-dianhydro D-sorbitol (isosorbide) and 2-ethyl-1,3-hexanediol (EHDO), and the diisocyanate 4,4'-methylene bis(phenyl isocyanate) (MDI) were provided by Sigma Aldrich Co.

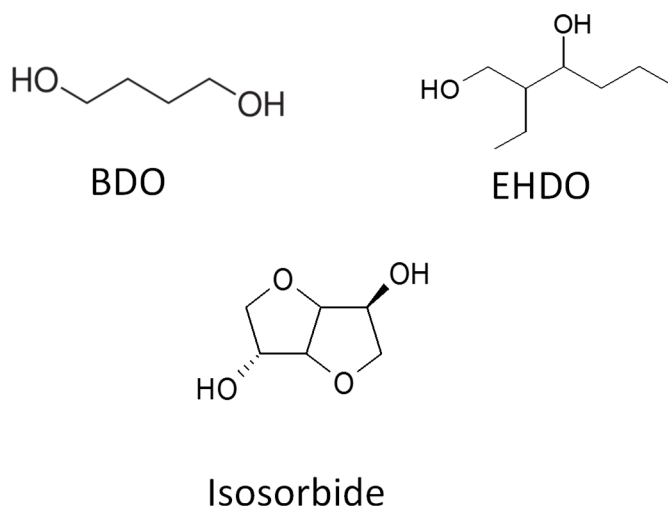


Figure 1. Chemical structure of the chain extenders used.

2.2. Synthesis and Processing

The procedure to synthesize the polymers has been described in a previous paper¹¹. A two-step procedure involving the formation of a polyurethane prepolymer was used^{25,26}. The first step consisted in adding the polyester polyol and a variable excess of MDI diisocyanate (in view of obtaining a constant final HS content of 13 wt%) in a 300 mL closed reactor at 80°C. The mixture was placed under nitrogen atmosphere and stirred at 600 rpm for 50 minutes. The precise required amount of chain extender BDO, isosorbide or EHDO was then added in the reactor with a syringe after being conditioned in an oven to lower the viscosity and the mixture stirred at 1,000 rpm during 1 minute, then at 600 rpm for about 10 minutes according to the viscosity changes.. The polymer was then put between two metallic plates under a hot press at 110°C under 40 bar pressure for 1 hour and cooled to room temperature to process a 2 mm-thick TPU film. The plates were covered with a silicone sheet in order to limit the material oxidation. Even though silicone is quite permeable to air, oxidation is still reduced, as shown by the light color of the plates obtained after pressing.

The procedure for the synthesis of MDI-EHDO and MDI-isosorbide model hard segments is the same as that described in an earlier work for MDI/BDO polymer¹¹. The polymers were synthesized by solution polymerization in a 250 mL flask in tetrahydrofuran. The reaction was catalyzed by 0.01 wt% dibutyltin dilaurate for 24 h under magnetic stirring at 65°C (reflux). After 24h, the obtained turbid solution was cooled down to room temperature under air before the addition of distilled water, which allowed the precipitation of the model hard segment. The

precipitated hard segment was washed with distilled water several times and filtered on a Buchner filter to obtain a white powder in the case of BDO and isosorbide HS, and a film for EHDO HS which was finally dried in an oven at 100°C for 4 h.

To prepare the bitumen-TPU blends, 100 g of 160/220 grade bitumen were placed in a metal pot and heated at 180°C for 1 h. Granules of TPU were added in the hot bitumen. Once the TPU was softened in the bitumen, the mixture was stirred at 2,500 rpm at 170°C for 15 minutes with a Rayneri agitator. The hot blend (“binder”) was poured on a silicon sheet which was placed between two metallic plates and pressed to obtain 2 mm-thick films that were then cooled down under ambient air to room temperature.

2.3. Instruments and methods

Dynamic mechanical analysis (DMA) was made in torsion mode on a homemade pendulum under inert atmosphere (helium) at 600 mbar from -120 to 130°C with a heating rate of 1 K.min⁻¹. The test was performed at a constant frequency of 1 Hz and low strain amplitude (10%) on parallelepipedic specimen (2 x 6 x 12 mm³).

Rheological properties of TPUs were measured using an ARES rheometer from TA Instruments Co. at 1 Hz from 80 to 180°C considering a plate-and-plate geometry (25 mm diameter, 2 mm gap) and 2% strain amplitude.

Differential scanning calorimetry tests were carried out using a Q20 TA Instrument calibrated with Indium. Hermetic aluminum pans were used to seal TPU samples of 5-7 mg which underwent a first cooling stage from room temperature to -80°C, followed by a heating ramp of 10 K.min⁻¹ up to 240°C. The specimens were submitted to a nitrogen flow rate of 50 mL.min⁻¹. The value of the glass transition temperature is given at the onset.

Protocols for determination of Hansen’ solubility parameters have been described elsewhere¹¹. The measurements were made using HSPiP® software²⁷ after testing the polymer solubility in various solvents (choosing an increment value of 1 for soluble situation and a value of 0 for non-soluble situation). The measurement was based on Hansen’s calculation of the solubility parameter and led to a three dimension (3D) diagram (δ_D = dispersive; δ_P = polar; δ_H = hydrogen bond) of solubility parameters with a solubility sphere of radius R_0 encompassing the good solvents for the considered compound.

Fluorescence microscopy tests were conducted using an optical microscope Zeiss equipped with a high pressure mercury UV lamp HBO in reflection mode with a two-filter system allowing to analyze specimens under 300-400 nm and 450-490 nm wavelength ranges. The polymer-modified bitumen samples were broken at low temperature in liquid nitrogen to allow analysis of the morphologies across the sample thickness. The fluorescence images obtained were segmented using the Fiji²⁸ software. The percentage of swollen TPU, which appears white in the images (due to the absorption of aromatic compounds), was then measured and averaged on at least five images. A swelling coefficient was then estimated as the ratio between the average surface fraction of TPU-rich phase measured in the images and the initial weight fraction of added polymer. Considering the close density values of bitumen and TPU, this coefficient is expected to be equal to 1 for non-swollen TPU, and >1 when swelling occurs.

Samples for transmission electron microscopy, TEM, were prepared by cryo-ultramicrotomy at -80°C on a UC7 Leica microtome device using two diamond knives, the first one for the pyramid preparation and the second for cutting slices of 100 nm thickness. Observations were conducted on a Philips CM120 at an acceleration voltage of 120 kV at ambient temperature.

Atomic force microscopy (AFM) was performed with a Dimension 3100 AFM device connected to a NanoScope V scanning probe controller (Bruker Instruments, Plainview, NY). All images were obtained at ambient temperature in tapping mode using a pointprobe-plus[®] silicon (PPP-NCH) from Nanosensors with a high resonance frequency (ca. 300 kHz). A lateral resolution of 3-5 nm can be achieved by this configuration with a vertical resolution of 0.5 nm. Very flat surfaces were obtained by cryo-ultramicrotomy, for this reason only phase images (highlighting a hard/soft contrast) after treatment with Gwyddion freeware²⁹ are shown in the present paper.

3. RESULTS AND DISCUSSION

3.1. Properties of the hard segments used to prepare the polymer

Thermal analysis was run on the model hard segments prepared with BDO, isosorbide and EHDO as chain extenders (Figure 2). The first scan highlights that only the hard segments MDI-BDO and MDI-isosorbide are semi-crystalline, with the presence of several melting endotherms at 172, 203 and 213°C for MDI-BDO¹¹, and 210 and 223°C for MDI-isosorbide, respectively. The second scan reveals the presence of a glass transition at 172°C for MDI-isosorbide hard segment, followed by a melting endotherm at 218°C. Literature reported higher glass transition temperatures of the model hard segments MDI-isosorbide, respectively 187°C for Cognet-Georjon *et al.*¹⁴ and 183°C for Marin *et al.*³⁰. For MDI-BDO, two melting endotherms are present at 203 and 217°C. Concerning MDI-EHDO hard segment, only a glass transition at 91°C is shown on both scans which is associated with the amorphous nature of this segment. Regarding the melting enthalpy of the semi-crystalline hard segments in the second scan, it could be concluded that MDI-BDO hard segment (enthalpy of 48.0 J.g⁻¹) exhibits a higher crystallinity than MDI-isosorbide hard segment (enthalpy of 13.8 J.g⁻¹). This assumption is confirmed by WAXS analysis (Figure 3) with a diagram showing well defined peaks for MDI-BDO, while only a sort of halo is present for MDI-isosorbide.

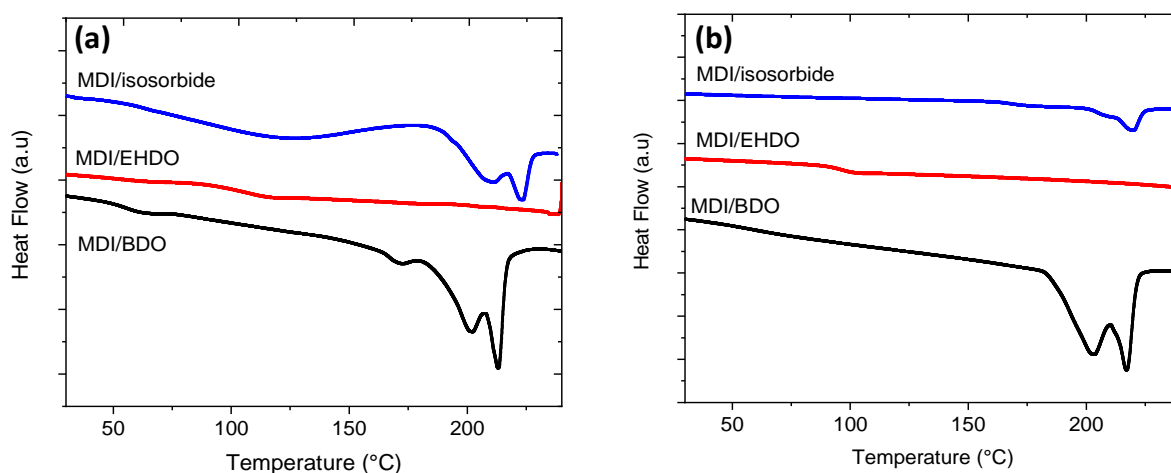


Figure 2. Differential scanning calorimetry thermograms of hard segments MDI-BDO, MDI-isosorbide and MDI-EHDO a) first scan; b) second scan.

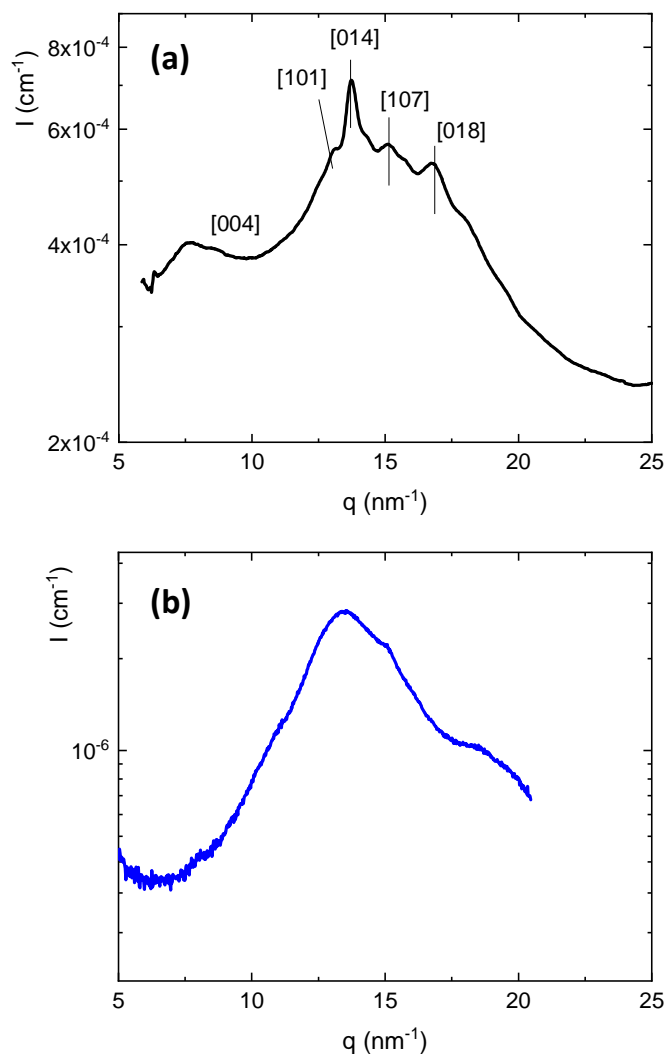


Figure 3. Wide angle X-ray scattering patterns of the semi-crystalline hard segments a) MDI-BDO with indexed peaks according to literature^{20,31,32} and b) MDI-isosorbide.

To go further, Hansen solubility parameters (HSP) were evaluated for the different hard segments used in this study through experimental solubility tests are described in section 2.3 and in more details in a previous article (from which are extracted HSP values for MDI-BDO)¹¹.

Table 2 shows the value of these solubility parameters and the sphere radius for the three hard segments. The obtained hydrogen components of HSP show a higher value for MDI-BDO and a lower value for MDI-EHDO, which agrees with the ability of BDO to provide a higher amount of hydrogen bonds than the secondary and asymmetrical alcohols. MDI-BDO and MDI-isosorbide hard segments show close HSP values, except that the radius of the solubility sphere is slightly higher for MDI-isosorbide, meaning that isosorbide based hard segments are more easily soluble. Regarding MDI-EHDO, lower HSP values are globally observed with a high

radius for the solubility sphere. These results are in total agreement with the ability of the studied hard segments to crystallize since MDI-BDO shows a higher crystallinity than MDI-isosorbide, and even more than MDI-EHDO that is fully amorphous.

Table 2. Hansen solubility parameters of the hard segments

Polymer	δ_{TOT} (MPa ^{1/2})	δ_D (MPa ^{1/2})	δ_P (MPa ^{1/2})	δ_H (MPa ^{1/2})	Sphere radius R_0 (MPa ^{1/2})
MDI-BDO	24.3 ± 1.5	18.2 ± 0.5	8.2 ± 1.7	13.8 ± 0.9	3.4
MDI-isosorbide	24.0 ± 0.5	18.0 ± 0.5	9.9 ± 0.6	12.4 ± 1.1	3.9
MDI-EHDO	21.5 ± 0.7	17.3 ± 0.3	7.7 ± 0.5	10.2 ± 0.5	5.9

3.2. Properties of the polymer used for the modification

Three thermoplastic polyurethanes containing 13 wt% hard segments based on different chain extenders were then used in this study. Thermodynamic compatibility between hard and soft segments (SS) was evaluated based on the HSP values obtained for the soft segment prepared with the polyol P3000 and MDI diisocyanate in our previous work¹¹ which led to experimental solubility parameters values of $\delta_D = 19.1 \pm 0.6$ MPa^{1/2}, $\delta_P = 4.2 \pm 0.9$ MPa^{1/2}, $\delta_H = 6.7 \pm 0.4$ MPa^{1/2}. Figure 4 shows the overlapping diagrams of the soft and hard segments solubility spheres. The calculated distance between centers of the solubility spheres of soft and hard segments is equal to 8.4 MPa^{1/2} for the TPU P3000-MDI-BDO, 8.4 MPa^{1/2} for the TPU P3000-MDI-isosorbide and 6.1 MPa^{1/2} for the TPU P3000-MDI-EHDO. The percentage of overlapping of the soft sphere with the hard segments sphere gives 0% for P3000-MDI-BDO, 2% for P3000-MDI-isosorbide and 22% for P3000-MDI-EHDO. Considering the criteria established by Hansen suggesting that above a distance of 8 MPa^{1/2} incompatibility occurs between two components, TPU P3000-MDI-BDO and TPU P3000-MDI-isosorbide provide complete incompatibility between soft and hard segments and thus high phase separation. It appears that the high crystallinity of MDI-BDO hard segments promotes phase separation and drives the thermodynamic equilibrium for this polymer¹¹. Furthermore, the percentage of overlapping of the spheres is consistent with the order of compatibility expected based on the distance. In the case of TPU P3000-MDI-EHDO the distance is lower than 8 MPa^{1/2}, suggesting that these hard segments are expected to present a partial compatibility with the soft phase. Based on the previous assumption, solubility distance for TPU P3000-MDI-EHDO suggests that the soft and hard segments are compatible, and given the amorphous nature of MDI-EHDO hard segment, limited or no phase separation is expected.

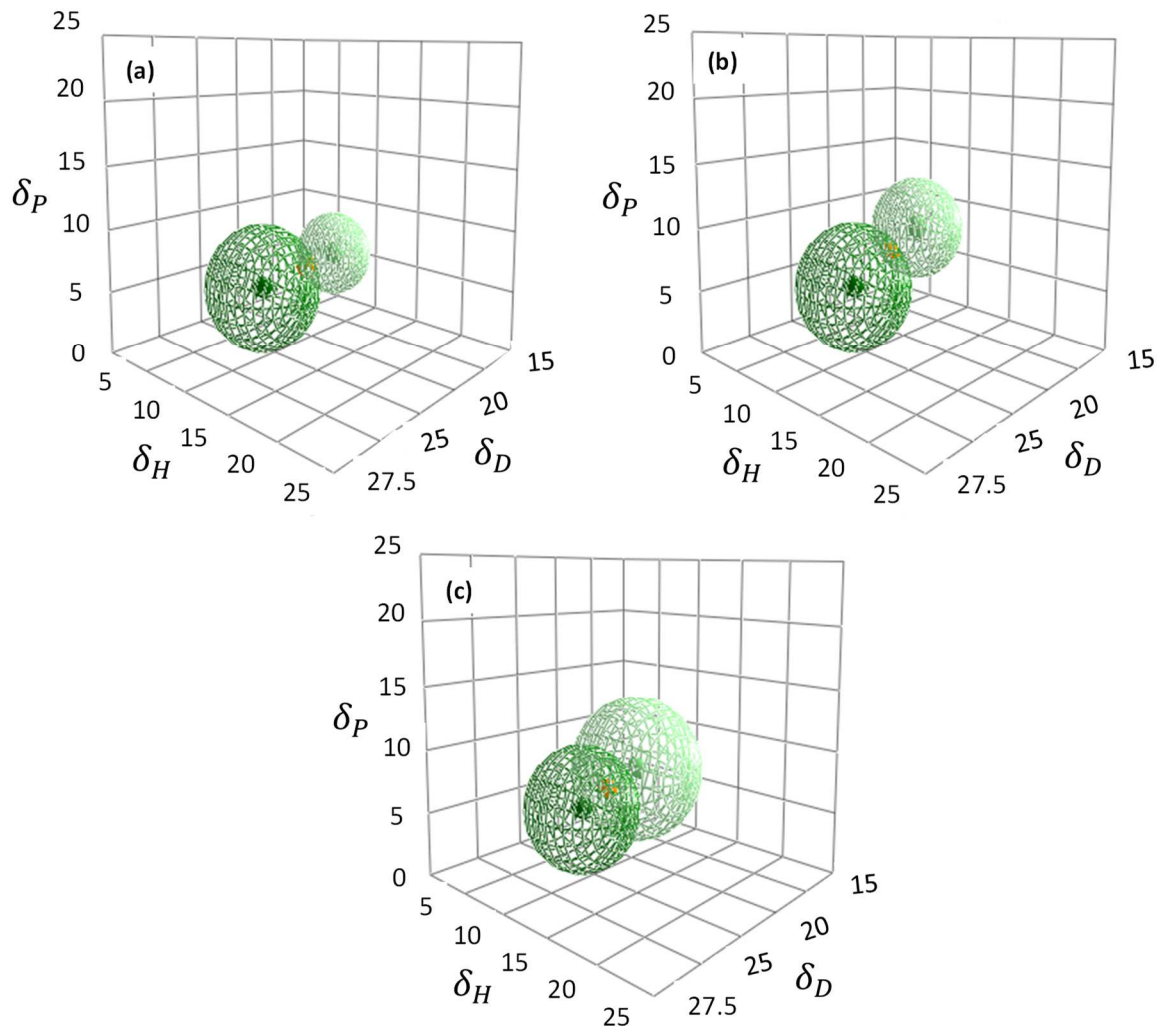


Figure 4. Solubility sphere diagrams in the 3D space ($\delta_D(\text{MPa}^{1/2})$; $\delta_P(\text{MPa}^{1/2})$; $\delta_H(\text{MPa}^{1/2})$) comparing solubility spheres of soft segments (green sphere) and hard segments (light green) prepared with a) MDI-BDO; b) MDI-isosorbide; c) MDI-EHDO.

Thermal properties of the polymers analyzed with differential scanning calorimetry (Figure 5) revealed at -54°C a glass transition for the soft segments of TPUs made with hard segments

based on BDO or isosorbide, while the TPU P3000-MDI-EHDO showed a glass transition at -49°C , thus a few degrees higher. Unlike P3000-MDI-EHDO, other phenomena occur at higher temperature for P3000-MDI-BDO and P3000-MDI-isosorbide; i/ close to 47°C for TPU containing BDO as chain extender, a phenomena often mentioned but not clearly explained in the literature, which could be associated either with the glass transition of separated and amorphous hard domains, or with the breakage of H-bonds^{11,33}; ii/ at high temperature small endothermal peaks between 170 and 190°C for BDO-based TPU, and a glass transition at 172°C for isosorbide-based TPU. On this basis, it is assumed that the latter corresponds to the glass transition of the amorphous MDI-isosorbide hard segments. In the case of P3000-MDI-BDO, the endotherms at high temperature are associated to the melting of well-organized hard segments, as it is well-known that MDI-BDO segments are semi-crystalline (Figure 2)^{11,14,23}.

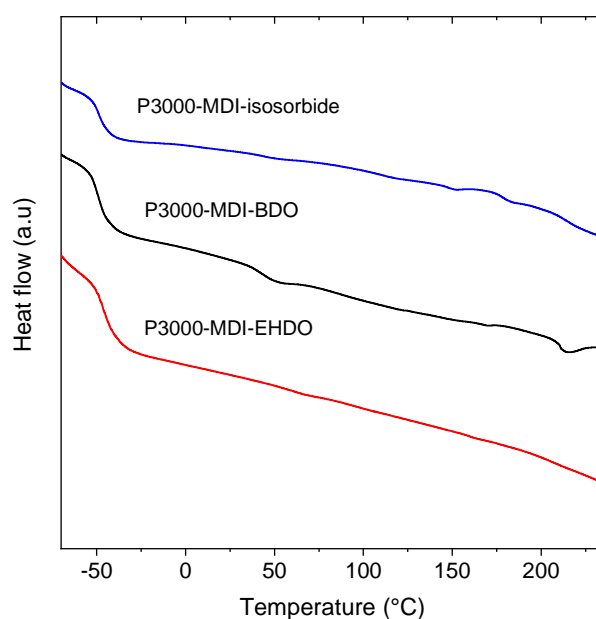


Figure 5. *Differential scanning calorimetry thermograms of the TPU P3000-MDI-chain extender containing 13 wt% hard segment content.*

The presence of several transitions for P3000-MDI-BDO and P3000-MDI-isosorbide associated to the soft and hard segments in the structure of the polymers confirms that phase separation occurs in these TPUs. In contrast for P3000-MDI-EHDO, the absence of any transition related to the hard segments and the increase in the low glass transition temperature suggests that this TPU is not phase-separated but rather composed of homogeneously mixed soft and hard segments.

Morphology investigation of the TPUs by TEM and AFM confirmed the phase separation in P3000-MDI-isosorbide, and the presence of only one phase in P3000-MDI-EHDO (that incidentally makes the sample too soft and sticky to achieve AFM observations with the tips used). (Figure 6). In the case of P3000-MDI-BDO, earlier studies using SAXS and AFM analyses have shown the phase separation in this TPU and that its microstructure can be described considering one soft phase made of polyol chains and short miscible hard segments and a hard phase organized as semi-crystalline nanodomains¹¹ (Figure 6a and Figure 6d). Finally, unlike P3000-MDI-BDO that is phase separated and semi-crystalline, P3000-MDI-isosorbide is amorphous and phase-separated, and P3000-MDI-EHDO is amorphous and homogeneous (Figure 7).

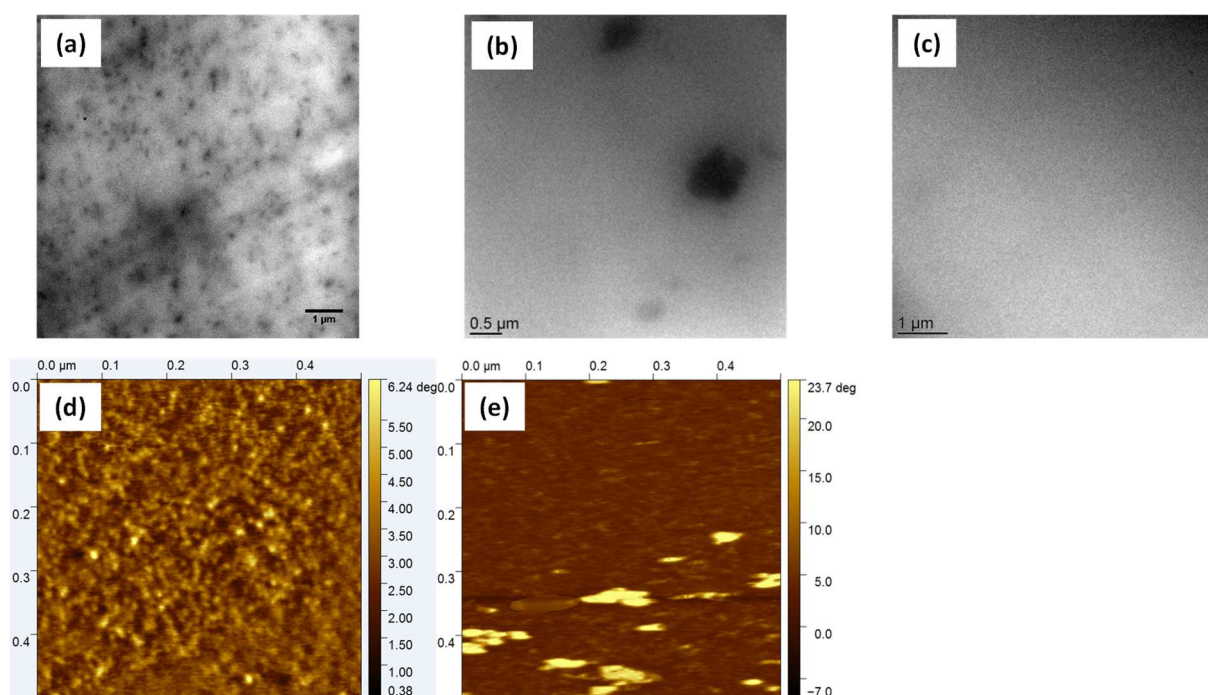


Figure 6. Microstructural analyses of the TPU P3000-MDI-chain extender containing 13 wt% of hard segments; a) TEM image of P3000-MDI-BDO; b) TEM image of P3000-MDI-isosorbide; c) TEM image of P3000-MDI-EHDO; d) AFM phase image of P3000-MDI-BDO; e) AFM phase image of P3000-MDI-isosorbide.

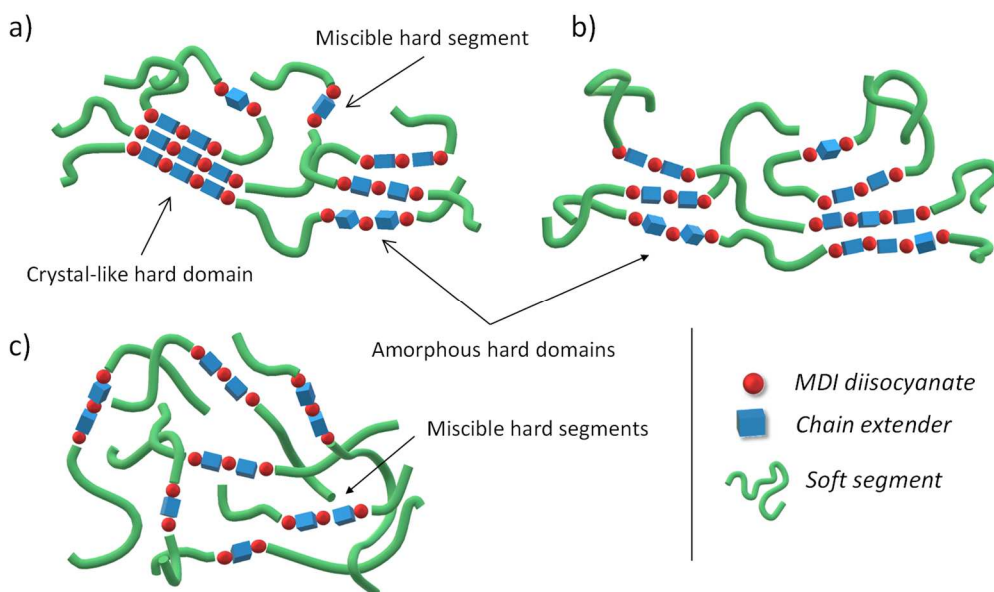


Figure 7. Scheme of the microstructures of the TPU as a function of the chain extender used
a) BDO; b) Isosorbide; c) EHDO.

Dynamic mechanical analysis of the TPUs (Figure 8) shows that the main relaxation associated to the glass transition of the polymers occurs close to -50°C for BDO and isosorbide based TPUs and about 10°C higher than the other polymers for EHDO based TPU, thus in agreement with thermal analysis (Figure 5). TPU P3000-MDI-EHDO flows right after the main relaxation while TPU P3000-MDI-BDO and TPU P3000-MDI-isosorbide present a rubbery plateau over a wide range of temperature before flow finally occurs at high temperature ($100\text{-}120^{\circ}\text{C}$). The difference of behavior is due to the presence of separated nanodomains of hard segments in BDO and isosorbide based TPUs, absent for P3000-MDI-EHDO, which act as physical crosslinking nodes in the soft segments continuous rich phase. These small hard domains in addition to physical entanglements confer to the materials a thermoplastic elastomer mechanical behavior by maintaining a high modulus up to the relaxation temperature of the HS, i.e. melting of the crystallized HS for P3000-MDI-BDO, and relaxation of the amorphous HS at 172°C for P3000-MDI-isosorbide.

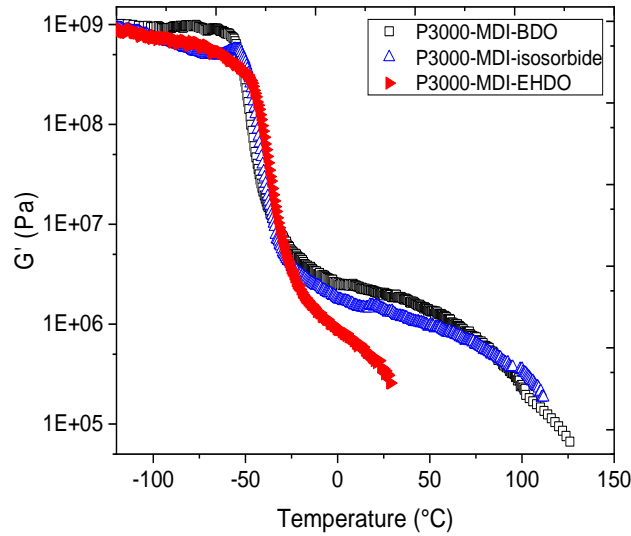


Figure 8. Dynamic mechanical analysis of the TPUs, storage modulus $G' = f(T)$.

3.3. Bitumen modification

The TPUs described above were mixed with bitumen to make blends containing 13 wt% of polymer. Fluorescence microscopy was used to analyze the morphology of the three blends (Figure 9). For this polymer content, only the blend prepared with TPU P3000-MDI-isosorbide gives a morphology containing a TPU-rich continuous phase (white phase) with dispersed bitumen-rich phase (dark phase), characteristic of phase inversion. In the case of the blend prepared with TPU P3000-MDI-BDO, co-continuous bitumen and TPU-rich phases are obtained while the blend with TPU P3000-MDI-EHDO presents a non-inverted morphology with a dispersed TPU-rich phase.

This result shows that even at low hard segment content (13 wt%), the nature of the hard segments and more precisely of the chain extender strongly impacts the morphology of the bituminous blend.

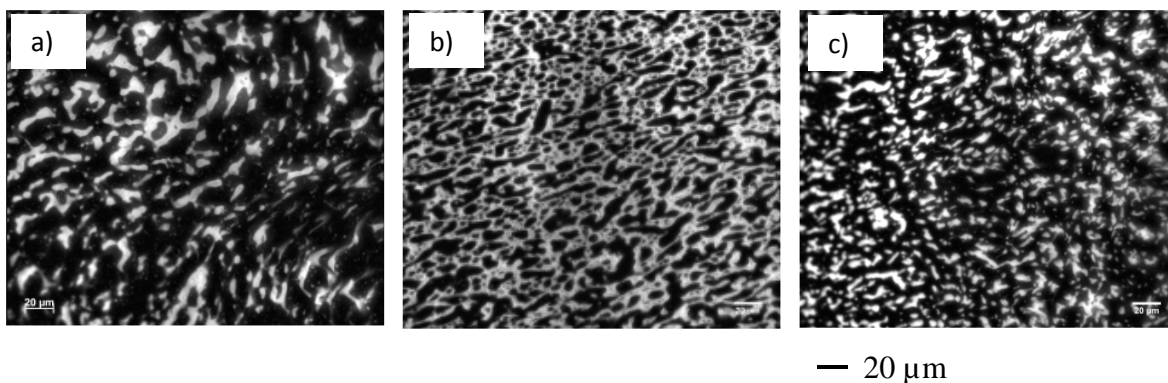


Figure 9. Fluorescence microscopy images of blends containing 13 wt% TPU made with a) P3000-MDI-BDO, b) P3000-MDI-isosorbide, c) P3000-MDI-EHDO.

An estimation of the swelling coefficient of the polymers was made based on fluorescence microscopy image analysis (Figure 10). TPU P3000-MDI-isosorbide seems to be the most swollen by bitumen, followed by TPU P3000-MDI-EHDO and finally by TPU P3000-MDI-BDO which shows the lowest swelling coefficient.

Hansen solubility parameters of the bitumen were evaluated in a previous work³⁴ and give solubility values of $\delta_D = 17.9 \pm 0.2 \text{ MPa}^{1/2}$, $\delta_P = 3.1 \pm 0.6 \text{ MPa}^{1/2}$, $\delta_H = 2.3 \pm 0.6 \text{ MPa}^{1/2}$. Solubility parameters of the bitumen were compared to those of the hard segments and the distance between centers of the solubility spheres was calculated (Table 3 and see supporting information Figure S 1).

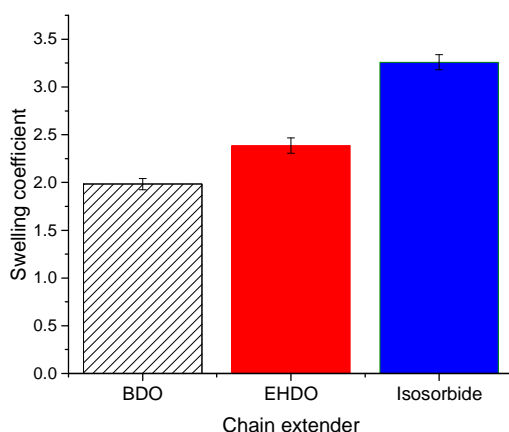


Figure 10. Swelling coefficient of the TPUs in bitumen as a function of their chain extender.

Table 3. Distance and percentage of overlapping between the solubility spheres of bitumen and the hard segments.

	Distance to bitumen sphere (MPa ^{1/2})	% of overlapping with bitumen sphere
MDI-BDO	12.1	0
MDI-isosorbide	12.2	0
MDI-EHDO	9.2	13

First, all the hard segments can be expected to show high incompatibility with bitumen, since the distances between centers of solubility spheres of bitumen and of the hard segments are all higher than 8 MPa^{1/2} (Table 3). As a consequence the hard segments are expected to be hardly swollen by bitumen³⁴. Based on those distance values, it is thus assumed that only the soft phase is responsible for the swelling observed in the polymer, as previously discussed in another work⁷. More generally, if the difference of swelling observed regarding the TPU used is only due to the composition of the soft phase, and knowing that every TPU is here composed of the same soft segments, made of the P3000 polyol and MDI diisocyanate, then finally the difference should originate only from the degree of hard segments soluble in the soft ones. HSP results have suggested that MDI-isosorbide and MDI-BDO hard segments were completely incompatible with the soft phase, with a high distance between centers of the solubility spheres and a percentage of overlapping of only 2% for MDI-isosorbide (Figure 4).

In the case of isosorbide which leads to both lower reactivity (due to its secondary hydroxyl groups) and amorphous hard segments, mobility is provided which allows the polymer to get complete phase separation thanks to thermodynamic incompatibility. As a result, while the presence of short MDI-BDO hard segments in the soft phase limits its swelling by bitumen, the absence of MDI-isosorbide hard segment in the soft phase allows the soft phase to be entirely and as much as possible swollen by bitumen. This high swelling gives rise to the observed morphology with a continuous TPU-rich phase.

For TPUs based on MDI-EHDO HS, a lower swelling coefficient is presumably due to the presence of mixed hard segments in the soft phase, as described with Hansen solubility diagrams (Figure 4) by lower solubility distances (< 8 MPa^{1/2}) and higher percentage of overlapping with the soft segments with 22% for MDI-EHDO. The presence of incompatible hard segments in the soft phase could explain the decrease of swelling observed for the soft phase as well as the resulting morphology, since a very highly swollen soft phase leads to co-

continuous morphology by fluorescence microscopy observations²⁴ (see supporting information in Figure S 2). Then, the study of the swelling of the different polymers highlights the presence of mixed hard segments in the soft phase and, combined with Hansen solubility parameters, confirms that distance values below $8 \text{ MPa}^{1/2}$ lead to partially compatible soft and hard segments, with a compatibility which can be estimated by the percentage of overlapping of the sphere. Thus, despite the semi-crystalline nature of the TPU P3000-MDI-BDO, which presents high phase separation thanks to the high crystallinity of MDI-BDO HS, small HS remain in the soft phase.

Rheological analyses were carried out on the different blends and show a general improvement in mechanical properties compared to the neat bitumen, with a higher modulus for the three blends but also a change in mechanical behavior (Figure 11). Overall, it is assumed that the mechanical properties of the blend are governed by the continuous or co-continuous TPU-rich phase. Indeed, plenty of works have shown the improvement in mechanical properties observed when changing a morphology with a dispersed polymer phase to a morphology with a co-continuous phase^{6,7,24}. The blend with P3000-MDI-EHDO shows a lower storage modulus than the others, explained by the homogeneous character of this polymer that flows after its main relaxation, and this blend has a permanently viscous behavior. For the blend made with P3000-MDI-isosorbide, an increase in storage modulus occurs compared to the previous blend, with the appearance of a viscoelastic behavior due to the thermoplastic elastomer nature of the used TPU (Figure 8), but also to the morphology of this blend (Figure 9) showing a continuous swollen soft phase containing amorphous incompatible MDI-isosorbide HS nanodomains. As discussed earlier²⁴, despite the continuous TPU-rich phase exhibited by P3000-MDI-isosorbide/bitumen blend a viscous behavior is still observed, and thus this specific morphology is not the only requirement to promote a change in mechanical behavior of the bituminous blend.

For the blend prepared with bitumen and P3000-MDI-BDO, the storage modulus increases once again and a change in mechanical properties occurs, highlighted by $\tan \delta < 1$. This shows that the blend with P3000-MDI-BDO behaves like a thermoplastic elastomer, with the appearance of a small rubbery plateau. The difference in mechanical behavior between the blends made with P3000-MDI-BDO and P3000-MDI-isosorbide comes from the higher swelling of P3000-MDI-isosorbide in bitumen. Indeed, the higher swelling of this polymer leads to a bulky TPU-rich phase but having a lower storage modulus. Our earlier work has already shown that high swelling resulting in a morphology with a continuous TPU-rich phase is not sufficient to induce

high mechanical properties, which is in agreement with this study²⁴. In addition, the nature of the nanodomains of hard segments, which are semi-crystalline in the case of P3000-MDI-BDO, and amorphous for P3000-MDI-isosorbide could also be part of an explanation.

As a result, it appears once again that the swelling of the soft phase of the polymer is the key parameter when designing polymer modified bitumen. Indeed, in the case of TPU, the choice of the HS nanodomains is of great importance since the compatibility between HS and SS could be a parameter to tune the degree of swelling of the soft phase and consequently govern the mechanical properties. Then, the physical state of the hard segment, i.e. semi-crystalline or amorphous, is a critical parameter for designing TPU-modified bitumen. A semi-crystalline or a well phase-separated polymer would rather be preferable to impart a thermoplastic elastomer mechanical behavior to the bituminous material, since the swelling can be adjusted with the HS content²⁴ (Figure S 2). Literature has pointed out the importance of the crystallinity of the hard domains in the polymer, with higher amounts of crystalline domains giving rise to higher elasticity for the blend⁸ (higher storage modulus and lower phase angle), which is in total agreement with this study. Nevertheless, it is worth mentioning that the polymer P3000-MDI-isosorbide revealed itself to be an interesting polymer for bitumen modification, which allows an effective swelling of the soft phase and consequently a morphology with a continuous TPU-rich phase for a lower amount of polymer compared to TPU P3000-MDI-BDO. In addition, it is well-known that the MDI-isosorbide HS is usually semi-crystalline^{14,23,30}, which suggests that a potential increase in hard segment content of P3000-MDI-isosorbide could lead to better mechanical properties for the corresponding blends, while maintaining good swelling by bitumen's light fractions.

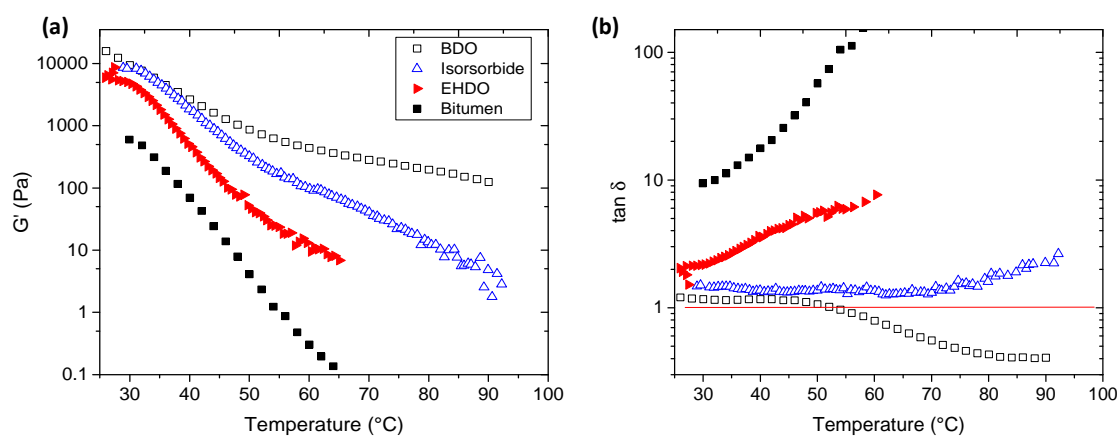


Figure 11. Rheological properties of the blend containing 13 wt% of TPU
a) storage modulus $G'=f(T)$, b) loss factor $\tan \delta=f(T)$.

CONCLUSION

In this study, we proposed to highlight the influence of polyurethane building blocks and specifically hard segment chemical nature on the properties of TPU-modified bitumen. By combining thermodynamic aspects using Hansen solubility parameters with thermal and swelling analyses, an explanation for phase separation in the polymer have been suggested by the ability of the hard segments to organize within crystalline structures. Three types of polymers were synthesized, semi-crystalline and phase separated, amorphous and phase separated, or amorphous and homogeneous. Although MDI-BDO based TPU is known to be well phase separated, the use of swelling coefficient of the polymer in bitumen highlights the presence of hard segments MDI-BDO trapped in the soft phase (P3000-MDI). In the case of MDI-isosorbide based TPU, these methods revealed full incompatibility between the HS and the P3000 based soft segments, which is consistent with Hansen solubility parameters results. The different nature of hard segments leads to different degree of mixing of the hard segments in the soft phase, and govern the way the polymer is swollen by the light fractions of bitumen and thus the morphology of the blend as well as its mechanical behavior. The presence of bitumen-incompatible HS in the soft phase allows to control its swelling by lowering it, which promotes blends with higher elasticity when using a thermoplastic elastomer.

ACKNOWLEDGEMENTS

The “Centre Technologique des Microstructures, plateforme de l’Université Claude Bernard Lyon 1”, CT μ and the Consortium Lyon Saint-Etienne de Microscopie (CLYM, FED 4092) are acknowledged for granting access to their equipments.

REFERENCES

1. Sengoz, B., Topal, A. & Isikyakar, G. Morphology and image analysis of polymer modified bitumens. *Constr. Build. Mater.* **23**, 1986–1992 (2009).
2. Redelius, P. Bitumen solubility model using hansen solubility parameter. *Energy and Fuels* **18**, 1087–1092 (2004).
3. Liang, M. *et al.* Thermo-rheological behavior and compatibility of modified asphalt with various styrene – butadiene structures in SBS copolymers. *Mater. Des.* **88**, 177–185 (2015).
4. Liang, M. *et al.* Rheological property and stability of polymer modified asphalt : Effect of various vinyl-acetate structures in EVA copolymers. *Constr. Build. Mater.* **137**, 367–380 (2017).
5. Schaur, A., Unterberger, S. & Lackner, R. Impact of molecular structure of SBS on thermomechanical properties of polymer modified bitumen. *Eur. Polym. J.* **96**, 256–265 (2017).
6. Lu, X. & Isacson, U. Modification of road bitumens with thermoplastic polymers. *Polym. Test.* **20**, 77–86 (2000).
7. Airey, G. D. Rheological properties of styrene butadiene styrene polymer modified road bitumens. *Fuel* **82**, 1709–1719 (2003).
8. Saroufim, E., Celauro, C. & Mistretta, M. C. A simple interpretation of the effect of the polymer type on the properties of PMBs for road paving applications. *Constr. Build. Mater.* **158**, 114–123 (2018).
9. Yilgör, I., Yilgör, E. & Wilkes, G. L. Critical parameters in designing segmented polyurethanes and their effect on morphology and properties: A comprehensive review. *Polymer* **58**, A1–A36 (2015).
10. Camberlin, Y. & Pascault, J. P. Phase segregation kinetics in segmented linear polyurethanes : Relations between equilibrium time and chain mobility and between equilibrium degree of segregation and interaction parameter. *J. Polym. Sci. Polym. Phys. Ed.* **22**, 1835–1844 (1984).

11. Gallu, R. *et al.* On the use of solubility parameters to investigate phase separation-morphology-mechanical behavior relationships of TPU. *Polymer (Guildf)*. **207**, 122882 (2020).
12. Bagdi, K. *et al.* Quantitative estimation of the strength of specific interactions in polyurethane elastomers, and their effect on structure and properties. *Eur. Polym. J.* **48**, 1854–1865 (2012).
13. Bonart, R. & Muller, E. H. Phase Separation in Urethane Elastomers as Judged by Low-Angle X-Ray Scattering. I. Fundamentals. *J. Macromol. Sci. Part B* **10**, 177–189 (1974).
14. Cognet-Georjon, E., Méchin, F. & Pascault, J.-P. New polyurethanes based on diphenylmethane diisocyanate and 1,4:3,6-dianhydrosorbitol, 1. Model kinetic studies and characterization of the hard segment. *Macromol. Chem. Phys.* **196**, 3733–3751 (1995).
15. Li, Y., Ren, Z., Zhao, M., Yang, H. & Chu, B. Multiphase structure of segmented polyurethanes: Effects of hard-segment flexibility. *Macromolecules* **26**, 612–622 (1993).
16. Cuvé, L., Pascault, J. P. & Boiteux, G. Synthesis and properties of polyurethanes based on polyolefin : 2 . Semicrystalline segmented polyurethanes prepared under heterogeneous or homogeneous synthesis conditions. *Polymer (Guildf)*. **33**, 3957–3967 (1992).
17. Blackwell, J., Nagarajan, M. R. & Hoitink, T. B. Structure of polyurethane elastomers. X-ray diffraction and conformational analysis of MDI-propandiol and MDI-ethylene glycol hard segments. *Polymer (Guildf)*. **22**, 1534–1539 (1981).
18. Xiang, D. *et al.* Multiphase Structure and Electromechanical Behaviors of Aliphatic Polyurethane Elastomers. *Macromolecules* **51**, 6369–6379 (2018).
19. Minoura, Y. *et al.* Crosslinking and mechanical property of liquid rubber. I. Curative effect of aliphatic diols. *J. Appl. Polym. Sci.* **22**, 1817–1844 (1978).
20. Blackwell, J. & Lee, C. D. Hard-segment polymorphism in MDI/Diol-based polyurethane elastomers. *J. Polym. Sci. Polym. Phys. Ed.* **22**, 759–772 (1984).

21. Cognet-Georjon, E., Méchin, F. & Pascault, J.-P. New polyurethanes based on 4,4'-diphenylmethane diisocyanate and 1,4:3,6 dianhydrosorbitol, 2. Synthesis and properties of segmented polyurethane elastomers. *Macromol. Chem. Phys.* **197**, 3593–3612 (1996).
22. Klinedinst, D. B., Yilgör, I., Yilgör, E., Zhang, M. & Wilkes, G. L. The effect of varying soft and hard segment length on the structure-property relationships of segmented polyurethanes based on a linear symmetric diisocyanate, 1,4-butanediol and PTMO soft segments. *Polymer (Guildf)*. **53**, 5358–5366 (2012).
23. Blache, H. *et al.* New bio-based thermoplastic polyurethane elastomers from isosorbide and rapeseed oil derivatives. *Ind. Crops Prod.* **121**, 303–312 (2018).
24. Gallu, R. *et al.* Rheology-morphology relationships of new polymer-modified bitumen based on thermoplastic polyurethanes (TPU). *Constr. Build. Mater.* **259**, 120404 (2020).
25. Delebecq, E., Pascault, J. P., Boutevin, B. & Ganachaud, F. On the versatility of urethane/urea bonds : Reversibility, blocked isocyanate, and non-isocyanate polyurethane. *Chem. Rev.* **113**, 80–118 (2013).
26. Prisacariu, C. *Polyurethane elastomers from morphology to mechanical aspects*. (Springer, 2011).
27. Abbott, S., Hansen, C. M. & Yamamoto, H. *Hansen solubility parameters in practice complete with eBook, software and data 5th edition*. (2013).
28. Schindelin, J. *et al.* Fiji: an open-source platform for biological-image analysis. *Nature methods* **9**(7). 676–682 (2012). doi:10.1038/nmeth.2019
29. Nečas, D. & Klapetek, P. Gwyddion: An open-source software for SPM data analysis. *Cent. Eur. J. Phys.* **10**(1), 181–188 (2012).
30. Marin, R., Alla, A., Martinez de Illarduya, A. & Munoz-Guerra, S. Carbohydrate-based polyurethanes: A comparative study of polymers made from isosorbide and 1,4-butanediol. *J. Appl. Polym. Sci.* **123**, 986–994 (2012).
31. Blackwell, J., Nagarajan, M. R. & Hoitink, T. B. Structure of polyurethane elastomers : effect of chain extender length on the structure of MDI / diol hard segments. *Polymer (Guildf)*. **23**, 950–956 (1982).

32. Born, L., Crone, J., Hesse, H., Müller, E. H. & Wolf, K. H. On the structure of polyurethane hard segments based on MDI and butanediol-1,4: X-ray diffraction analysis of oriented elastomers and of single crystals of a model compound. *J. Polym. Sci. Polym. Phys. Ed.* **22**, 163–173 (1984).
33. Balko, J. *et al.* Clarifying the origin of multiple melting of segmented thermoplastic polyurethanes by fast scanning calorimetry. *Macromolecules* **50**, 7672–7680 (2017).
34. Gallu, R. *et al.* Investigating compatibility between TPU and bitumen SARA fractions by means of Hansen solubility parameters and interfacial tension measurements. *Constr. Build. Mater.* **289**, (2021).

SUPPORTING INFORMATION

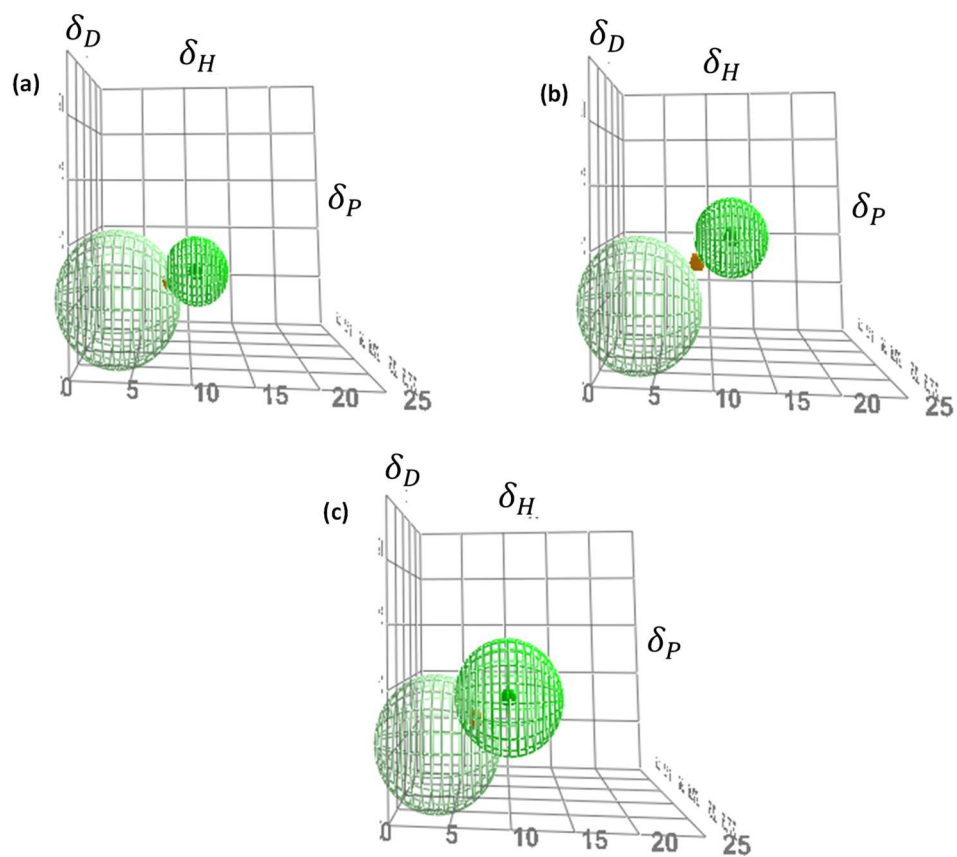


Figure S 1. Hansen solubility diagrams comparing solubility spheres of bitumen (light green) and hard segments a) MDI-BDO; b) MDI-isosorbide; c) MDI-EHDO.

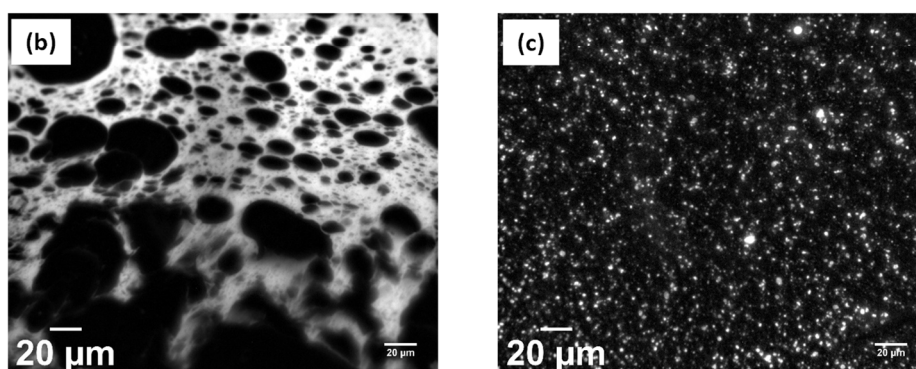
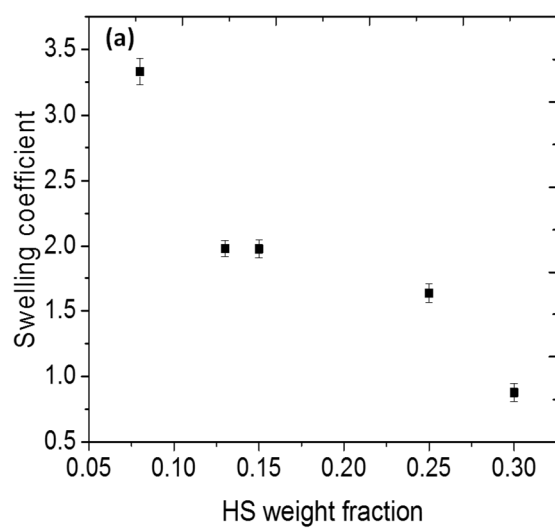


Figure S 2. a) Swelling coefficient diagram of the TPU P3000-MDI-BDO as a function of hard segment (HS) content; b) Fluorescence microscopy images of the bitumen-TPU blend made with a TPU at low HS content (8 wt%); c) Fluorescence microscopy images of the bitumen-TPU blend made with a TPU at high HS content (30 wt%).